Elevation over Azimuth Position Controller

Prepared by:

Thomas Davies

Fourth-Year Electrical Engineering Student

University of Cape Town

19th October 2004

File: Thesis.lyx

Document No: 4028

Document Rev: A

Declaration

I declare that this project report is my own, unaided work. It is a project report submitted to the Department of Electrical Engineering, University of Cape Town, in partial fulfilment of the requirements for the degree of Bachelor of Science in Engineering. It has not been submitted before for any degree or examination in any other university.

Signature of Author . . . .

Cape Town 19th October 2004

Abstract

This project concerns the design and implementation of an elevation over azimuth position controller for a Navy Jammer pedestal. The position controller system is implemented on a Cogent CSB337 Single Board Computer using position resolvers to provide position information. The position controller accepts digital position commands moves the pedestal to the appropriate position.

Acknowledgements

Contents

List of Figures

List of Tables

List of Symbols

θ	—	I
K	—	Motor gain
T_m	—	Mechanical time constant
E_f	—	Field Voltage
ω	—	Reference signal frequency
$ω_{shaft}$	—	Shaft frequency
V_R	—	Peak reference voltage

Glossary

Azimuth—Angle in a horizontal plane, relative to a fixed reference, usually north or the longitudinal reference axis of the aircraft or satellite.

Elevation—Angle in a vertical plane, relative to a fixed reference, usually the horizontal plane.

Interrupt—An event that interrupts normal processing and temporarily diverts flow-of-control through an interrupt service routine.

Pedestal—The structure which supports an antenna.

Rotor—The rotating armature of a motor or generator.

Selsyn—A system that consists of two or more motor-like devices that are intended to sense or control shaft position.

Servo-motor—The area on earth covered by the antenna signal.

Stator—The stationary part of a motor or generator in or around which the rotor revolves.

Transducer—An electrical device that converts one form of energy into another.

Chapter 1

Introduction

1.1 Subject of this report

This document concerns the design, implementation and testing of an elevation over azimuth position controller for a Navy electronic warfare (EW) jammer pedestal using a single board computer (SBC). The requirement for this project is that the antenna on the pedestal has to be moved by the position controller to a specific position or in a search pattern as input to the SBC.
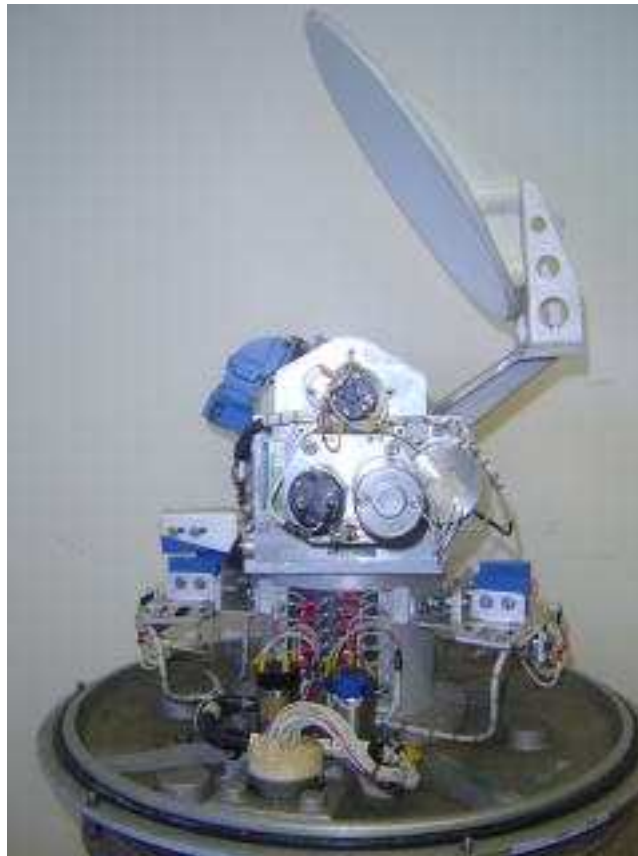
Figure 1.1: Navy EW Jamer Pedestal

1.2 Background to Study

The University of Cape Town has a Navy EW jammer pedestal for experimentation as can be seen in figure 1.1. The pedestal has two axes of movement: the horizontal (or azimuth axis), and the vertical (or elevation) axis. Since the elevation axis is closer to the antenna than the azimuth axis, the pedestal is known as an *elevation over azimuth* pedestal. The pedestal uses 28 volt direct current (DC) motors to move the antenna in each axis. The position of each axis is measured using position resolvers, and the rate at which the antenna is moving is measured using tachogenerators.

The requirement of this project is to create a controller that will move the antenna to specific positions as input to the SBC. The movement has to be accurate, take as short an amount of time as possible and the position has to be maintained without minimal deviation.

1.3 Objectives

The objective of this project is to create a position controller with the equipment available that will move the position of the antenna in a manner optimised for speed and accuracy. The inputs are either of the following:

- Elevation and azimuth position

- Search pattern[1]

The position controller is based around a SBC, with the digital control algorithm implemented in software.

The project was divided into the following tasks:

1.3.1 Examination of the Pedestal Hardware and Interface Design

The first task in this project was to examine the characteristics of the components already on the pedestal and to test which of the components were still functional. As most of the documentation for the electronics on the pedestal is unavailable, electrical characteristics of certain components had to be measured to derive specifications. Once a better understanding of all the equipment is gained, a mathematical model for the position control process could be derived, and a hardware interface to the controller could be designed.

---

[1]Such as *nodding* or *raster*

Circuitry needed to be built which ensured that input signals and power supplies to the various components did not exceed operating specifications. Output from the position resolvers had to be converted from an analog signal to one which could be used by the digital components of the position controller. The motors required circuits which drove them at varying torque according to a reference signal. The rate information from the tachogenerators had to be fed back into the motor drive circuit within an inner rate loop.

1.3.2   Selection of a Platform for the Digital Control System

A decision between a PC and a single board computer had to be made, and due to the real time requirements a Cogent CSB337 single board computer was used as the platform for the position controller.

The CSB337 is a highly integrated SBC with a number of useful interfaces, devices and software tools that make it suitable for embedded control applications. The hardware devices include RS-232 Serial Ports for communication, Ethernet interface for network connection and Inter Integrated Circuit (I^2C) bus and serial peripheral interface (SPI) for device connectivity. The SBC has 8 MBytes of SDRAM to store data and programs in during operation and 32 MBytes of Flash memory for non-volatile storage of data or programs.

The CSB337 has a bootloader (MicroMonitor) pre-installed to load software into memory as it boots up and to initialise system registers.

A decision had to be made on whether to install an operating system on the SBC or to write stand-alone software. It was decided that it would be best to install an operating system and different types of operating systems where examined. A toolchain was created to enable software and an operating to be compiled for the SBC.

The real time operating system that is used is SnapGear Linux, which is based on uClinux. It can be run as a Real Time Operating System (RTOS) and comes with a number of packages. Applications and kernel modules were designed to test interfaces and peripherals on the single board computer.

1.3.3   Designing and coding the software

Universal Modelling Language (UML) class and data-flow diagrams were used to design the software in a top-down approach. The highest level was broken down into smaller pieces and described in UML. This process was repeated for each smaller section until there were three layers of hierarchy. C and C++ headers were generated from the UML class diagrams and the working code was generated based on the headers. The kernel modules were written in C, and the position controller application written in C++.

1.3.4 Interfacing the hardware to the software

An interface was designed to integrate the hardware and software in a stable and coherent manner. Tests were done to ensure the voltage levels were correct at the inputs and outputs. Kernel modules were tested to ensure that the circuits work correctly, and the actual response of each component was compared to the desired response. Designs were modified and adjusted to optimise performance and the expected error in each device was calculated and then measured.

1.3.5 Evaluating System Response and Deriving a Control System

With all the circuits and components functioning correctly the response of the system was measured and the parameters of the mathematical model for the system were calculated. The mathematical model described the manner in which the inputs affect the systems output and was used to design a controller. The controller was then implemented.

1.3.6 Overall Testing

Although testing was done at the end of each the tasks where possible, the overall system was tested and the results recorded and interpreted. Position commands were input to the system and the time and accuracy of the response was measured. The overall system was found to have an accuracy of 42 arc minutes.

1.4 Limitations and Scope

The focus of this report is not to create the best possible design for a position controller, but to create an accurate and efficient controller with the equipment at hand.

This project covers many different areas, including; hardware design, analog and digital interfacing, real time operating systems and embedded application programming. Due to the time constraints, not all areas could be examined in great detail, and would benefit from more exploration in the future.

1.5 Plan of Development

Chapter 2 gives a conceptual overview of the position controller system.

Chapter 3 is a background to the hardware on the pedestal.

Chapter 4 describes the interface to the hardware on the pedestal

Chapter 5 is a description of the software

Chapter 6 discusses the results obtained from the system

Chapter 7 makes conclusions based on those results and gives recommendations based on those conclusions

Chapter 2

Position Control Concept Overview

The method of controlling position is a closed loop control system as represented in figure 2.1. A sensor provides information about the current state of the process and a comparator compares the measured state to the desired state and outputs an error signal. A controller produces a driving output based on this error signal.
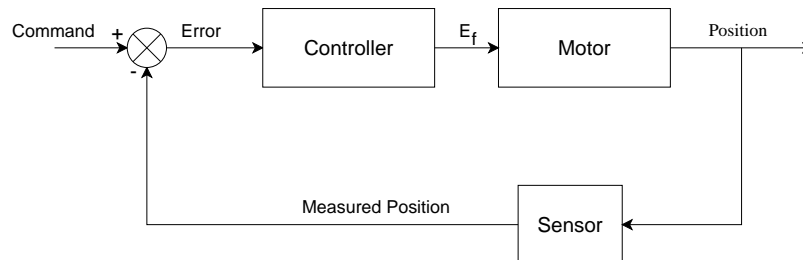
Figure 2.1: Typical Position Control Loop System

In the position controller system on the navy pedestals there is feedback information about the current motor rate provide, therefore a rate loop can be installed on the system as in figure 2.2.

The digital position control loop would then be closed around this rate loop and the overall position controller is shown in figure 2.3

The overall transfer function of a position control of this type has the form of equation 2.1, [22].

$$G(s) = \frac{K}{s(s+\alpha)} \tag{2.1}$$
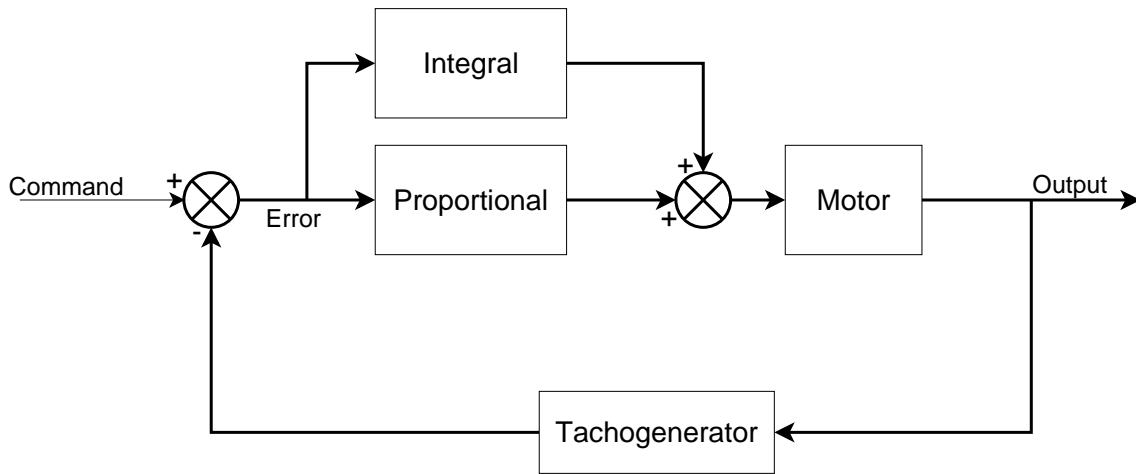
Figure 2.2: A Motor Rate Control System
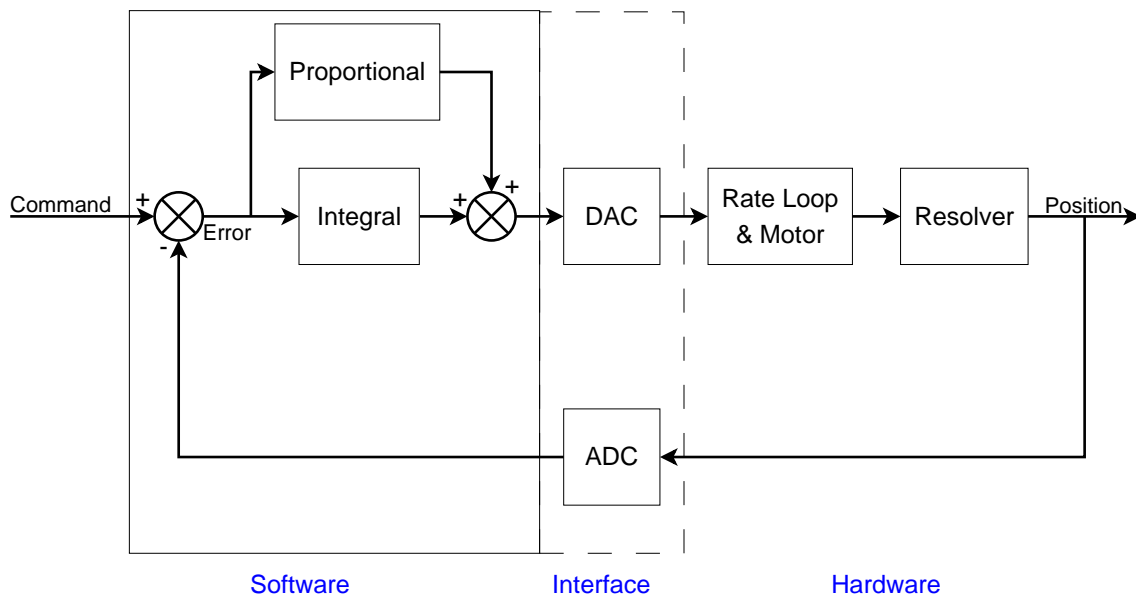
Figure 2.3: Position Controller Control Loop

The parameters of this model will be calculated by the methods described in [17] and [23].

Chapter 3

Background to the Hardware on the pedestal

This chapter is a description of the hardware components on the pedestal that relevant to this project. The concepts involved in the components are described in detail where applicable, along with the methods of operation. Each component is described individually.

3.1 Synchro Control Transformers

A synchro control transformer (CT) is a form of angular transducer. CTs are rotating transformers that output an analogue voltage that is uniquely related to the input shaft angle. A CT consists of a rotor with one winding which revolves around a stator with 3 windings in wye format, 120 degrees apart. The internal wiring is demonstrated in figure 3.1.

A CT accepts input voltage across the stator terminals as desribed in equation 3.1 [20, 15, 6].

$$
\begin{aligned}
\text{S1--S3} &= \sin \omega t \sin \theta \\
\text{S3--S2} &= \sin \omega t \sin(\theta + 120^o) \\
\text{S2--S1} &= \sin \omega t \sin(\theta + 240^o)
\end{aligned}
\tag{3.1}
$$

The rotor windings will then only produce a voltage across their terminals if the shaft input on the CT is not at angle θ. This output voltage is an error signal which can be fed into a phase sensitive detector and an error amplifier to produce a signal that will drive a motor to the correct position, and thus provide a servo control system.
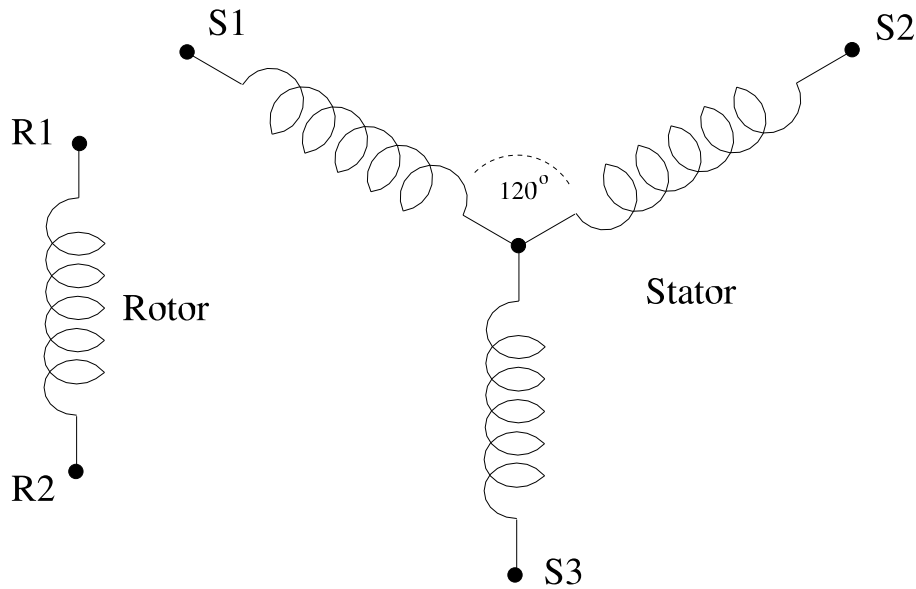
Figure 3.1: Internal Design of Synchro Control Transformer

3.2   Position Resolver Transmitters

Position resolver transmitters (TX) are angular transducers similiar in design to synchro control transformers in that they consists of rotor which rotates inside a stator. A TX outputs an analogue voltage that is uniquely related to its input shaft angle [9], just as a synchro control transformer does. A TX however has two rotor windings at 90 degrees angle to each other and two stator windings also seperated by a 90 degree angle. The internal wiring of a TX is shown in figure 3.2.

There are two common methods to calculate the shaft angle using position resolvers:

3.2.1   Excitation of rotor windings

If an alternating current is introduced across one of the rotor windings, a voltage is induced in the stator windings. Since the stator windings are at right angles to each other, the amplitudes of the voltages induced are related by the sine of cosine of the shaft angle [20, 15]. If the stator windings are excited with a signal:

$$A \sin \omega t \tag{3.2}$$

The output of the stator windings will be:

$$\text{S1--S3: } V_x = V_R \sin \omega t \sin \theta$$
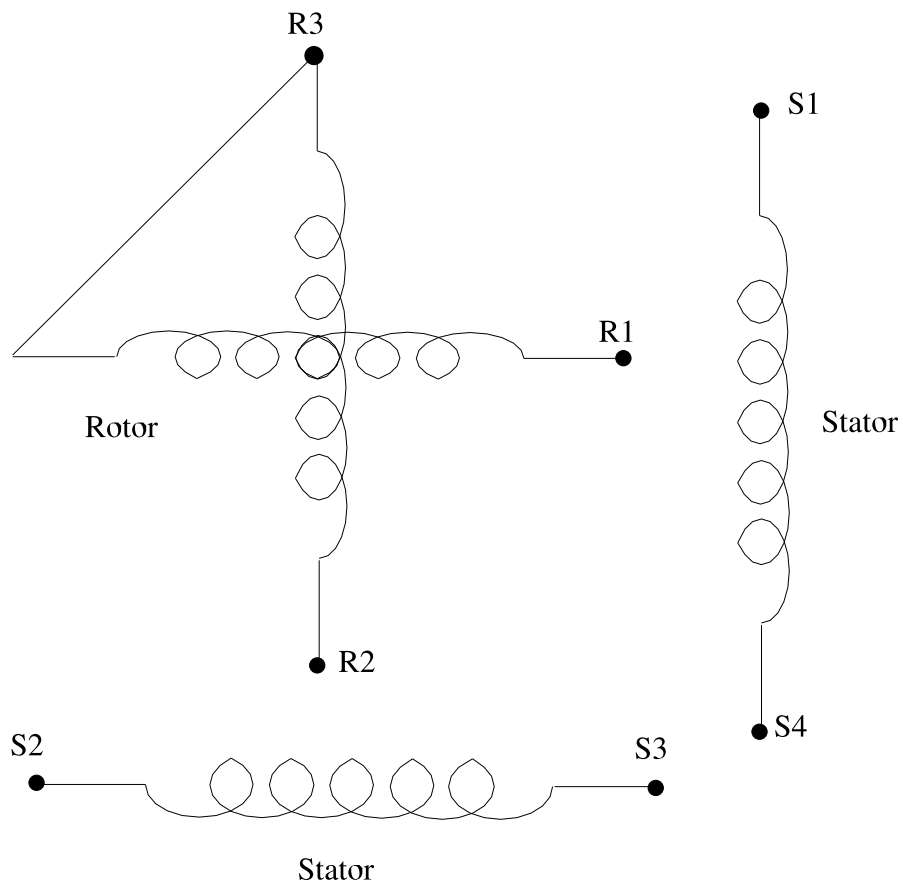
Figure 3.2: Internal Structure of a Resolver Transmitter

$$\text{S2--S4: } V_y = V_R \sin \omega t \cos \theta \tag{3.3}$$

Therefore, according to [15] the shaft angle θ can be determined by:

$$\theta = \arctan \frac{V_x}{V_y} \tag{3.4}$$

The output of a CT is shown in figure 3.3

(a) Shaft at 0 degrees

(b) Shaft at 90 degrees

(c) Shaft at 180 degrees

(d) Shaft at 270 degrees
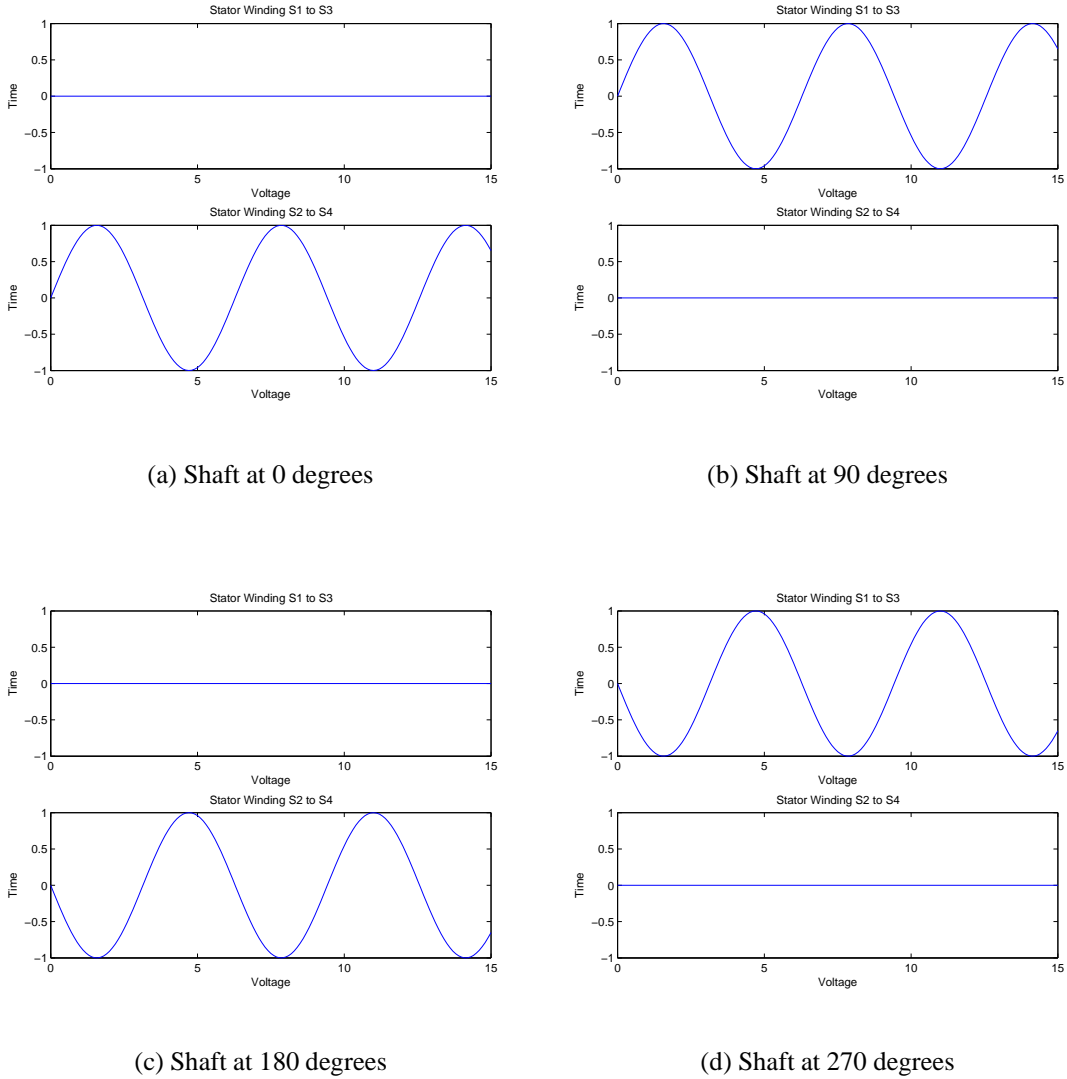
Figure 3.3: Output Signals of Position Resolver for Varying Shaft Angles

3.2.2 Excitation of stator windings

By exciting the two stator windings with two signals in phase quadrature to one another, the voltage induced on the rotor winding will have a fixed amplitude and frequency, but will have a phase that varies according to shaft angle θ [20, 9]. The input signals will be:

$$V_{S1--S3} = V_R \sin \omega t$$

$$V_{S2--S4} = V_R \sin(\omega t + 90^o) = V \cos \omega t \qquad (3.5)$$

The voltage induced across the rotor winding will be:

$$V_{R1--R2} = V_R \sin(\omega t + \theta) \qquad (3.6)$$

The phase of the signal across the rotor winding will range from 0° to 360° when compared to the reference signal and can be measured to determine the shaft angle.
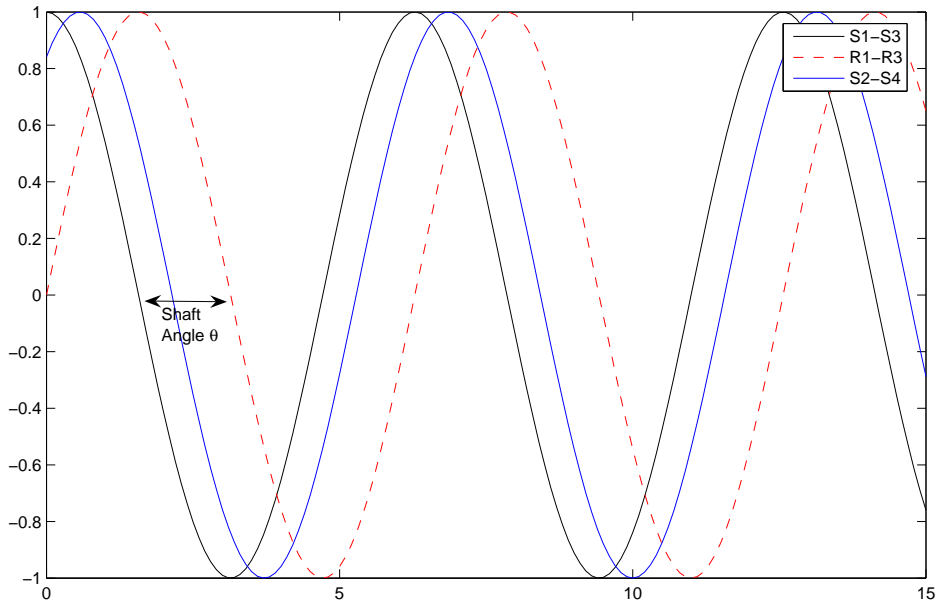
Figure 3.4: Signals on Position Resolver with Stator Excitation

3.2.3 Reference Frequency

The output of the resolver with a rotating shaft will be a modulated carrier signal of the form:

$$V_{output} = \sin(\omega_{shaft}t)V_R \sin(\omega t) \qquad (3.7)$$

In order to ensure that the correct angular information is conveyed, the reference frequency must always be greater than the shaft rotational frequency [9].

13

3.3   Tachometric Generators

Tachometric generators (tachogenerators) are transducers which convert rotational velocity into voltage. The tachogenerators used in this project were Servo - Tek SA - 740A -2 and provided an output of 7 Volts (V) for every 1000 revolutions per minute (RPM).

3.4   Direct Current Brushed Motors

The pedestal is moved by two direct current (DC) brushed motors that operate from -28 V to 28 V. The model type is Vactric 15P203, which has a maximum current rating of 0.95 Amps. The maximum rated speed is 5000 revolutions per minute (RPM) with a torque of 220 grams per centimeter.

3.5   Brake

There is a brake on the elevation axis to prevent uncontrolled movement in the system. The brake is disengaged when a voltage greater than 24 V is applied.

Chapter 4

Interfacing with the hardware

This chapter examines the methods used in interfacing to the components on the pedestal in detail, describing the specifications of the components and the associated interface. Calculations are made to determine optimal parameters for the interface and methods of improving accuracy are explored where relevant.

4.1   Synchro Resolver

The original design for this particular pedestal was an analogue position controller that made use of synchro control transformers and synchro control transmitters. In the original design the desired position was set by means of a synchro control transmitter and the synchro control transfomer provided feedback information based on the position of the shaft.

The synchro control transformers on this pedestal require three phases of 115 V from line to line at 400 Hertz (Hz) as an input to operate. The phases must be generated as described in equation 3.1. The output of the synchro control transformer is an alternating signal 90 V root-mean-squared (RMS).

Navy and Airforce craft commonly use 400 Hz power supplies since 400 Hz generators tend to be smaller and more efficient than more common 50 Hz generators [6]. However a 400 Hz power supply is not a common type of power supply and at the time of this project only one 400 Hz generator was available at the University of Cape Town which was still being tested.

A second disadvantage of using synchro resolvers is that with the high voltages required for operation, integration with digital equipment is difficult and requires special hardware, which is expensive. It was decided that since position resolvers can provide similar or improved accuracy [20], the synchro control transformers would not be used in this project, and be replaced by position resolvers on the pedestal .

4.2   Position Resolver Conversion

The position resolver output is in the form of two alternating signals described in equation 3.3. To calculate the shaft angle θ from this output, the amplitudes of the two signals need to be calculated. Since the shaft angle is related to the ratio of these two amplitudes (equation 3.4), either the peak value or the root-mean-squared (RMS) value can be used to determine it.

4.2.1   Measuring Position Resolver Output Signals

Two analogue-to-digital converters ADCs were used in order to measure the different output signals simultaneously. The ADCs used in this project are Texas Instruments ADS7824 CMOS 12 bit ADCs. The relevant characteristics are shown in table 4.1.

Table 4.1: Relevant ADS7824 ADC Specifications

Parameter	Specification
Resolution	12 bits
Maximum Sampling Frequency	40kHz
DC Accuracy	1 LSB
Analogue Input Range	-10 V to 10V
No. of Channels	4
Data Output Coding	Two's Complement

Since the 12bit ADCs operate from -10V to 10V, the least signicant bit (LSB) corresponds to:

$$\frac{20}{2^{12} - 1} = 0.00489\text{V} = 4,89\text{mV} \tag{4.1}$$

The ADC has no internal provision for correcting the internal bipolar zero error, but is guaranteed to be below a level slightly more than two LSBs. The specifications guarantee that the error between channels will be less than one LSB, and since the measurement required is a ratio of two channels, the zero offset error can be ignored. Therefore the error in calculating the ratio of two voltages will be a maximum of one LSB or 4,89 mV.

According to the specifications in table 4.1, the DC error is LSB, when added to the error between channels the maximum total error becomes:

$$e_{adc} = 2\text{LSB} = 9.78 \text{ mV} \tag{4.2}$$

The circuit used for the ADCs makes use of the Texas Instruments *TAG* feature [10],

which allows two ADCs to share input and output signals to minimise the use of data lines.

Precautions need to be taken to avoid noise on the ADC circuit and the following methods of eliminating noise were investigated:

Grounding Planes

Noise from digital signals causes large amounts of interference with the analogue-to-digital conversion process [1]. To avoid this the analogue and digital grounding planes were seperated and a decoupling capacitor was introduced between them.

Analogue Filtering

A possible method for removing noise is the introduction of an analogue filter before the input to the ADCs. However, an analogue filter implemented here can be implemented as a digital filter after the conversion process, without any heat sensitivity or non-linear response associated with some analogue devices [21].

Averaging of Samples

One of the most common methods for noise reduction is the averaging of a number of samples [1]. This is effectively a low-pass filter and every time the number of samples is doubled there is a reduction in noise by a factor of the square root of two.

The Goertzel Algorithm

The output signals from the position resolver are alternating signals at the same frequency as the reference signal in equation 3.2. Therefore all other frequency components are irrelevant and can be ignored. Since the only valuable information in those signals is the amplitude of the signals at the reference frequency, a possible solution would be to calculate the Discrete Fourier Transform (DFT) of those signals and examine the co-efficients of that frequency.

To calculate the DFT the Goertzel algorithm is used because it is more efficient that the fast Fourier Transform (FFT) when $\log_2 N$ co-efficients are required [12], and in this case only one co-efficient is required.

The Goertzel algorithm is a Infinite Impulse Response (IIR) filter which is defined by equation 4.3. It is implemented in the form of a second order filter as shown in figure 4.1

$$H(z) = \frac{1 - W_N^k z^{-1}}{1 - \left(\left(W_N^k - W_N^{-k} \right) z^{-1} + z^{-2} \right)} \tag{4.3}$$
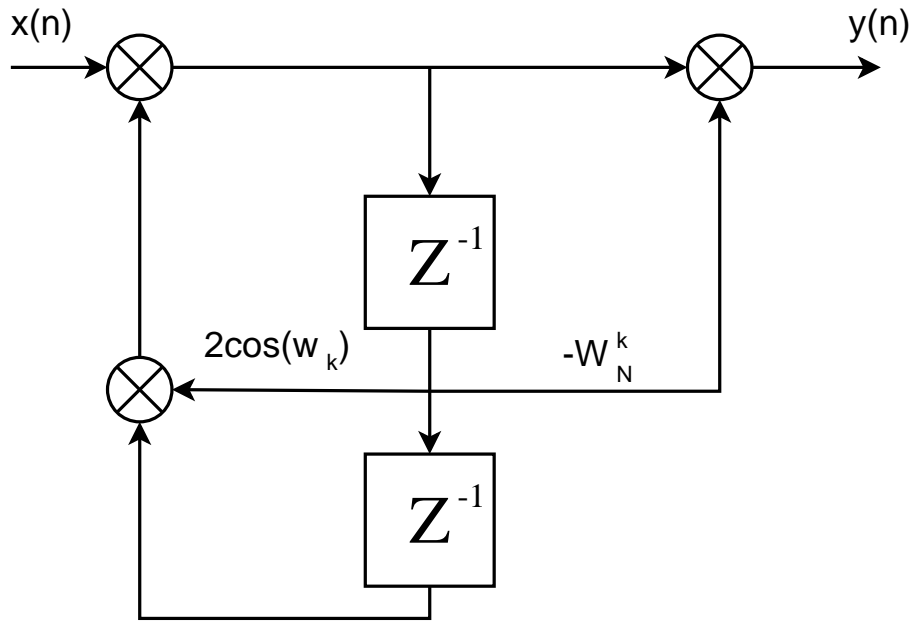
Figure 4.1: The Goertzel Algorithm as a Second Order Filter

The effect of the Goertzel algorithm is that of a very high Q-factor band-pass filter which removes most of the noise from the ADC input.

4.2.2 Input Reference Signal

The position resolvers on the pedestal are rated to accept an alternating current (AC) input of up to 10 Volts at 10 kHz. The full input voltage range is used to minimise noise. This range also allows the ADCs to be operated across their full range, without any need for voltage conversion.

The reference frequency, f_{ref}, to be used had to be less than the maximum rated frequency and was determined by two criteria, namely:

1. The maximum sampling rate of the ADC circuit.

2. The maximum shaft rotation speed on the pedestal.

The maximum sampling frequency, f_s, of the ADC circuit was conservatively estimated at at 20kHz based on specifications, and later measured at 17,54kHz in chapter 7. According to the Nyqist-Shanon sampling theorem [19, 21], the reference frequency has to be:

$$2f_{ref} < f_s \qquad (4.4)$$

Therefore the reference frequency must be less than 8.770 kHz.

The maximum shaft rotation was tested by measuring the number of rotations per minute that the pedestal could acheive when driven at full rate. This was found to be 14.83 revolutions per minute. Therefore the maximum shaft rotation frequency is:

$$2\pi (14.83) 60 = 5591.96 \text{ rad.sec}^{-1} \qquad (4.5)$$

According to equation 3.7, this would require the reference frequency be greater than 5591.96 rad.sec^{-1} or 889.8 Hz.

This result meant that the reference frequency had to lie within the following range:

$$889.8 \le f_{ref} \le 8770 \text{ Hz} \qquad (4.6)$$

With higher frequencies more succeptable to noise interference, it was decided to use a reference frequency of 1kHz.

A standard function Hewlett Packard 33120A function generator is used to generate the reference frequency for the position resolvers.

4.3   Movement of the Pedestal

The position controller has an digital rate command that needs to converted into an analogue current to the motor. The digital signal is converted by two digital-to-analogue converters, one for each axis.

4.3.1   Digital to Analogue Conversion

The DACs used in this project are Texas Instruments 12bit TLV5616 Digital to Analogue Converters. The DACs have an output range from 0 V to $2V_{ref}$, where V_{ref} can be from 0 V to 3.5 V. In this project V_{ref} is set at 3 V to avoid saturating the DAC in case of fluctuating voltage supplies, while still provide a good voltage range. Therefore the output range of the DAC is in the range of 0 V to 6 V.

4.3.2   Motor Drive Circuit

To move the pedestal the primary movers need to be supplied with a voltage in the range of -28V to 28V depending on the desired movement rate and direction required. The motor drive circuit used is provided by 4-Sight Optronics, based on a ST Microelectronics L292 Switch-Mode Driver, and accepts an input of the range -15V to 15V, which corresponds to an output to a motor in the range of -28 V to 28 V.

However, the input to the drive circuit is a unipolar DC voltage from the DACs in the range of 0 to 6 Volts. Therefore this voltage needs to be offset and amplified so the input to the motor drive circuit reflects the ranges described in table 4.2. This can be acheived by equation 4.7 and is implemented by means of a classic differential amplifier [11] with a gain of 5.

$$V_{out} = 5(V_{in} - 3) \qquad (4.7)$$

Table 4.2: Motor Drive Command Conversions

Output from DAC	Input to Motor Driver Circuit	Input to Motor
0 V to 3 V	-15 to 0V	-28 to 0V
3V	0 V	0 V
3 V to 6 V	0 V to 15V	0 V to 28 V

4.3.3   Tachogenerator interface

The rate information provided by the tachogenerator is connected through a voltage buffer to the motor drive circuit. This provides feedback for the inner rate loop, and is added to the error signal before the PI process of the position controller.

Chapter 5

Platform for the Position Controller Software

This chapter describes the digital portion of the position controller, in particular the platform on which the software will be run. The embedded device used for this project is described, along with the method used in running software on it. A simple application is then used to test the software creation process. The operating system used for this project is then described.

5.1 The CSB337 Single Board Computer

The University of Cape Town has recently purchased a number of Cogent CSB337 Single Board Computers (SBC) and one of which was made available for use in this project. The CSB337 is manufactured by Cogent Computer Systems, Inc. and is centered around an ARM920T Core, namely the Atmel AT91RM9200 microprocessor. The CSB337 has many highly integrated components on-board and the features applicable to this project are examined in further detail as follows:

Figure 5.1: The Cogent CSB337

5.1.1 Important Components on the CSB337

RS-232 Serial Port

Basic communication is provided between the SBC and other data terminal equipment (DTE), such as a PC, through this serial port. As the SBC is started the first RS-232 serial port (*uart 0*) is monitored for communication by the bootloader software, *MicroMonitor*. *MicroMonitor* provides basic control over the SDC through this serial port.

32 M-byte S-DRAM

The SBC has provide sufficient memory to load user programs or other data into on startup. This memory is volatile and the contents is lost when the power is disconnected.

8 M-byte Strata FLASH

Non-volatile storage space is provide to store software or in absence of power. This memory also holds the startup file, *monrc*, which can be configured to perform certain tasks on startup.

Ethernet Interface

A 10/100 M-Bit Ethernet interface is provided via internal Media Access Control (MAC). This allows connections to networks and fast transfer of data to and from the SBC.

5.1.2   The CSB300CF Break-out Board

The break-out board provides the following connectors for the CSB337.

- An Ethernet RJ45 connector for connecting to 10/100 Ethernet.

- DB9 connector for RS-232

- 5 Volt DC power connector

5.2   Running Software on the CSB337

Software can be written directly for the CSB337 in a variety of different programming languages. The software for this project is written in C and C++, cross-compiled on a Linux machine for a ARM processor.

To cross-compile for ARM, a toolchain is required to compile and link the C/C++ code into an executable that can run on a ARM machine. The toolchain used in this project is described in section 5.2.1.

5.2.1   Arm-Linux Toolchain

A precompiled uClinux arm-linux toolchain[1] was used to compile applications directly
for the CSB337. The toolchain installed and compiled application for the ARM machine
without any significant problems.

5.2.2   *Hello World* **Program**

To test the CSB337 and the *arm-linux* toolchain, a simple *hello world* application[2] was
compiled using the toolchain. The Gnu Complier Collection (gcc) version information
was:

```
gcc version 2.95.3 20010315 (release)(ColdFire patches - 20010318 from
http://fiddes.net/coldfire/)(uClinux XIP and shared lib patches from http://www.snap
```

Once the *hello world* application had been cross-compiled and linked it had to be copied
to SBC, this is acheived by using *MicroMonitor*

5.2.3   MicroMonitor

A null modem cable connected to the SBC's *uart0* RS-232 serial port provides basic
communication to a PC or other DTE. Using a terminal interface program called *minicom*
and communicating with the parameters described in [2], basic communication with the
SBC using MicroMonitor was possible.

The *hello world* application was transfered into the SBC's Strata Flash using Trivial File
Transfer Protocol (TFTP) via the Ethernet interface. The application was then executed
and the returned succesfully.

5.3   Embedded Operating System

SnapGear Linux is used as an embedded operating system (EOS) on the SBC. The SnapGear
distribution of Linux is based on uClinux and comes with a variety of packages. The ver-
sion used in this project was compiled with the GNU C library (glibc).

The main reason for using an EOS in this project is the layer of abstraction it provides
between the position controller software and the underlying system hardware. This is
shown in figure 5.2.

---

[1]Downloaded from http://www.snapgear.org `http://www.snapgear.org`
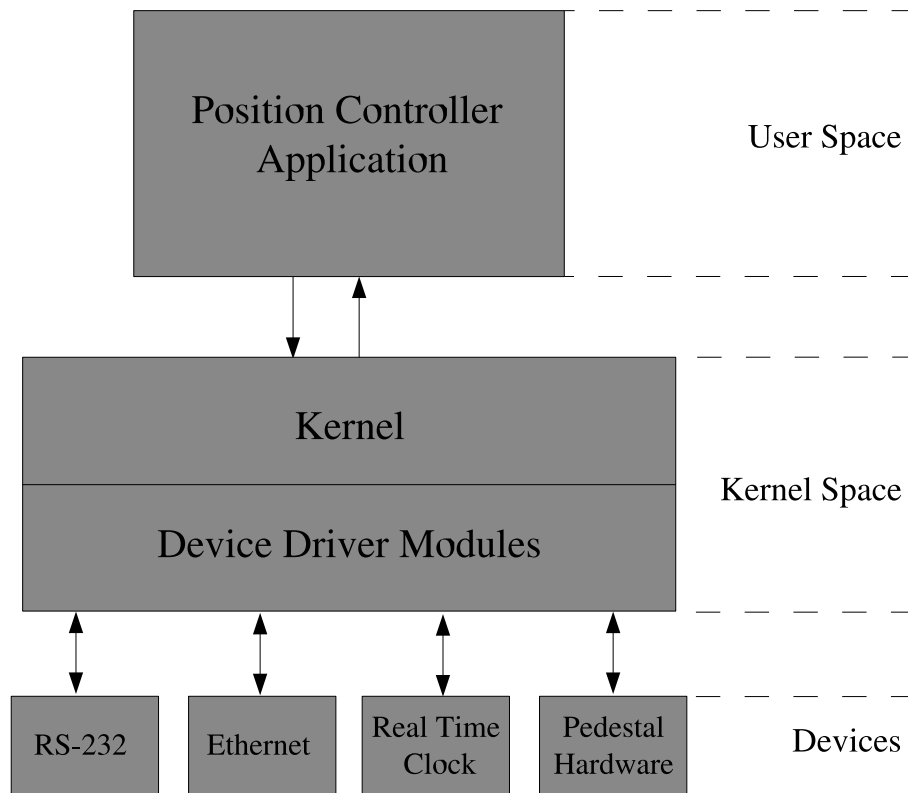[2]provided by Simon Winberg

Figure 5.2: Abstraction Layers of an Operating Systems

Linux is not a real-time operating system but provides performance which is acceptable to *soft* real-time systems [16], such as a position controller.

Chapter 6

Software to Control the System

This chapter describes the overall design of the software used in the position controller, beginning with the flow of data through the software. The different objects in the software are then described in the Unified Modeling Language as in [14]. Sequence and flow information about the software is presented in the form of a flowchart and a UML sequence diagram. Finally the methods used in testing the software are introduced.

6.1 Overall Design

6.1.1 Data Flow of the Software

Figure 6.1 is a data-flow diagram which demonstrates the basic interaction of the user, the software and the hardware. The diagram consists of the external entities; the pedestal interface, and the interface on the client machine and the main process; the position controller. The client machine presents the position controller with a request for a new position, and the position controller process ensures that the motor is given the correct rate information to drive the pedestal to the desired position.

Figure 6.2 demonstrates how the position controller software is broken down into smaller processes and data storage points, and the internal data flow is demonstrated. There are three main processes at this level which interact with one another through data stores, to ensure that they are weakly coupled.

The data-flow diagram in figure 6.3, demonstrates how the controller class calculates motor rate information from resolver position feedback and the desired position input.
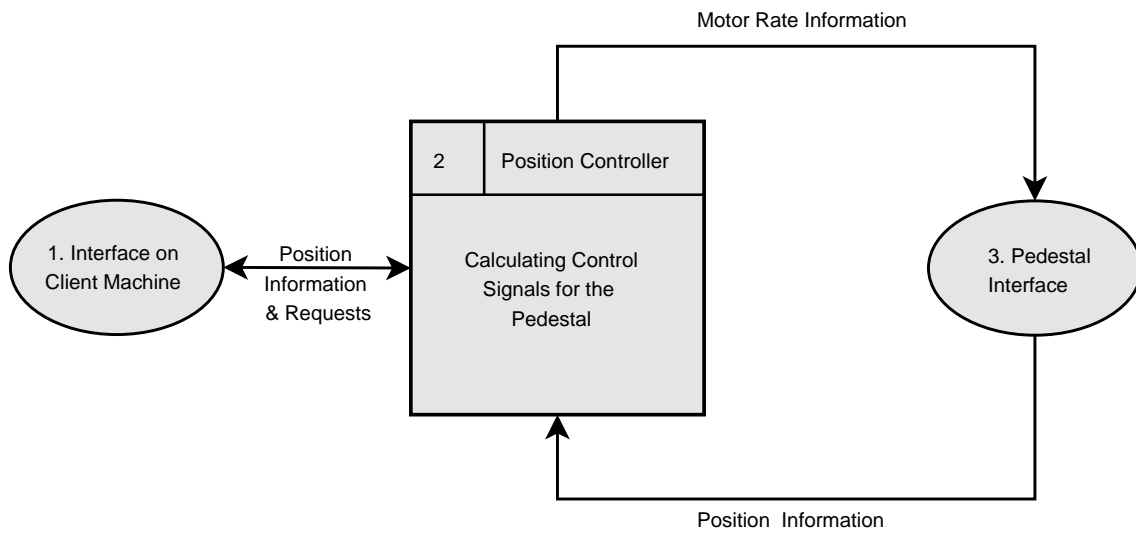
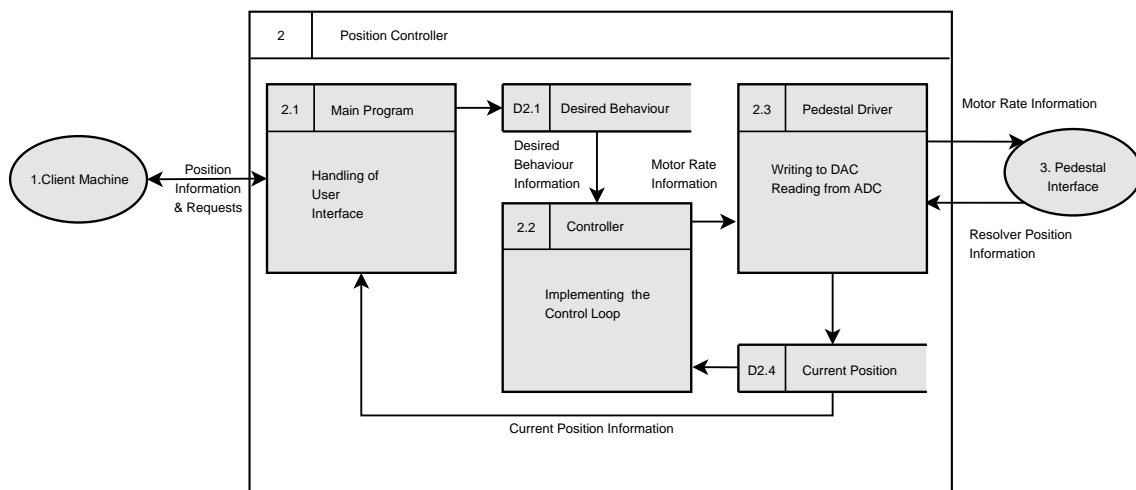Figure 6.1: Data-flow Context Diagram of Position Controller

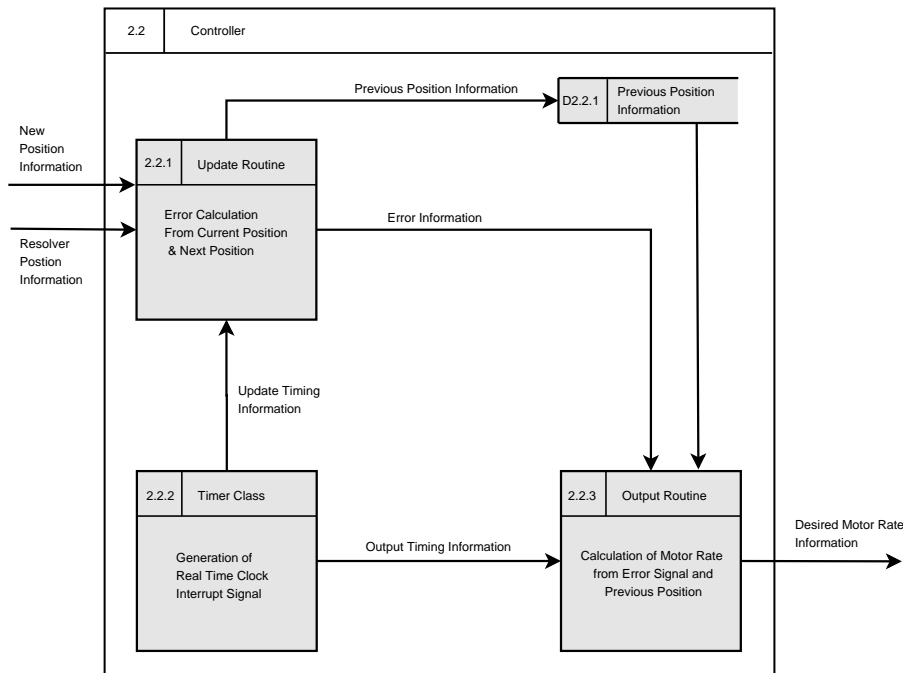Figure 6.2: Data-flow Level 1 Diagram of Position Controller

Figure 6.3: Data-flow Diagram of Controller Class

6.2 Objects in the Position Controller Software

The most important elements in the software are described in the following section. The software objects are described in UML by means of class diagrams.
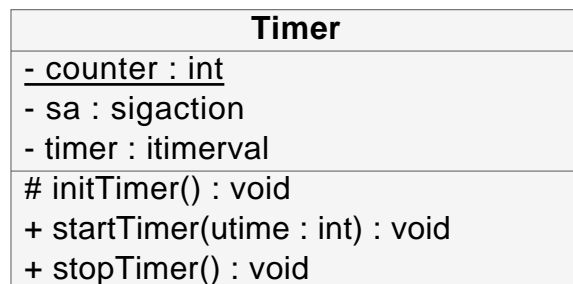
6.2.1 The Timer Class

Figure 6.4: Class Diagram of Timer Class

Figure 6.4 s the UML class diagram for the Timer Class. The Timer Class makes use of the Linux System Clock to measure time down to the microsecond level. The timer is started with a interval time specified in microseconds, and an interrupt service routine (ISR) to run every time the timer generates an interrupt.

PedestalDriver
+ devname : char
+ read() : string
+ write(buffer : string) : void

Figure 6.5: Class Diagram of Pedestal Driver Module

6.2.2   The Pedestal Kernel Module

The pedestal driver module as seen in figure 6.5 is a kernel module that runs in the kernel memory space. It is a driver for a character device, and creates a file enter in the '*/dev/*' directory of the operating system called */navy/0*. User-space applications can then open this device as if it were a file, to read and write to it.

Reading from the Pedestal Kernel Module

When a 'read' operation is called on the '*/dev/navy/0*' the driver module calls a function which reads from the ADC, and stores the value in a string of characters. The 'read' function handles all communication with the ADC circuit and needs no input from the user. The string returned by this function contains two signed integer values separated by a comma. These two values correspond to the different windings on the position resolver. The range of the output is from -2048 to 2047, which correspond to inputs to the ADC of -10V to +10V.

Writing to the Pedestal Kernel Module

A 'write' operation takes as a parameter an array of characters to be transmitted to the DAC. This array is converted to an unsigned integer lying within the range of 0 to 4095. 0 will translate to an output voltage of 0 Volts on the DAC and 4095 will translate to an output of 6V.

6.2.3   The Controller Class

In figure 6.6, the methods and attributes of the Controller Class are given. The public methods that are used are *getPosition()* to display the current position and *setPosition()* to set the new position. The *update()* function is called whenever the Timer Class generates a timeout interrupt and runs the designated ISR.

The controller class implements the control system for each and calculates new values every time the *update()* function is called. Therefore two instances of Class Controller are initialised, one for the elevation plane, and one for the azimuth plane.

Controller
- hemisphere : int
- iMax : float
- iMin : float
- iState : float
- pGain : float
- position : float
convertPos(buffer : string) : void
+ getPosition() : float
# setRate(rate : int) : void
+ update() : void
+ setPosition(new_position : float) : void

Figure 6.6: Class Diagrams of Controller Class

6.3 Sequence of Events in the Position Controller Software

To describe the logical flow of the software a flowchart, figure 6.7, is included. This flowchart demonstrates the typical operation of the position controller. The flow begins with a user input requesting a new position, and remains in a constant cycle until the system is shutdown.

Since this system is a real-time system, figure 6.8 is a UML sequence diagram and includes estimated latency or run-times at each process step.

6.4 Software Testing

6.4.1 Pedestal Kernel Module

Read Function

The *read* function was tested by attaching a variable power supply to the ADC and varying the voltage supplied from -10 Volts to 10 Volts. The function was called at -10V, 0 V 10 V and a number of other random voltage levels. The ADC was then grounded and 1000 conversion cycles were initiated and the results recorded.

Write Function

The *write* function was tested by attaching the DAC to an oscilloscope and varying cycling through the entire range of permissible DAC input codes. The output voltage on the oscilloscope was recorded and compared to the input code.
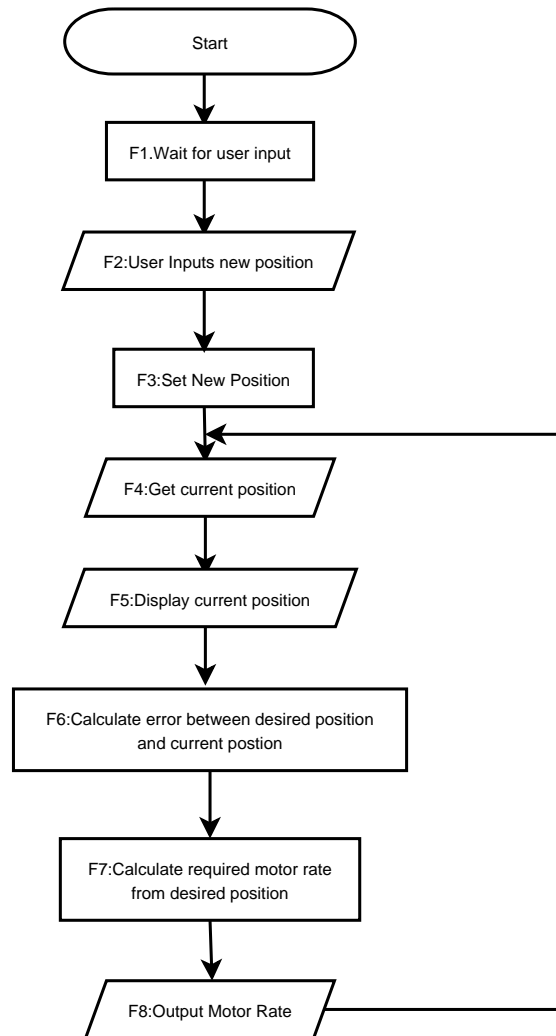
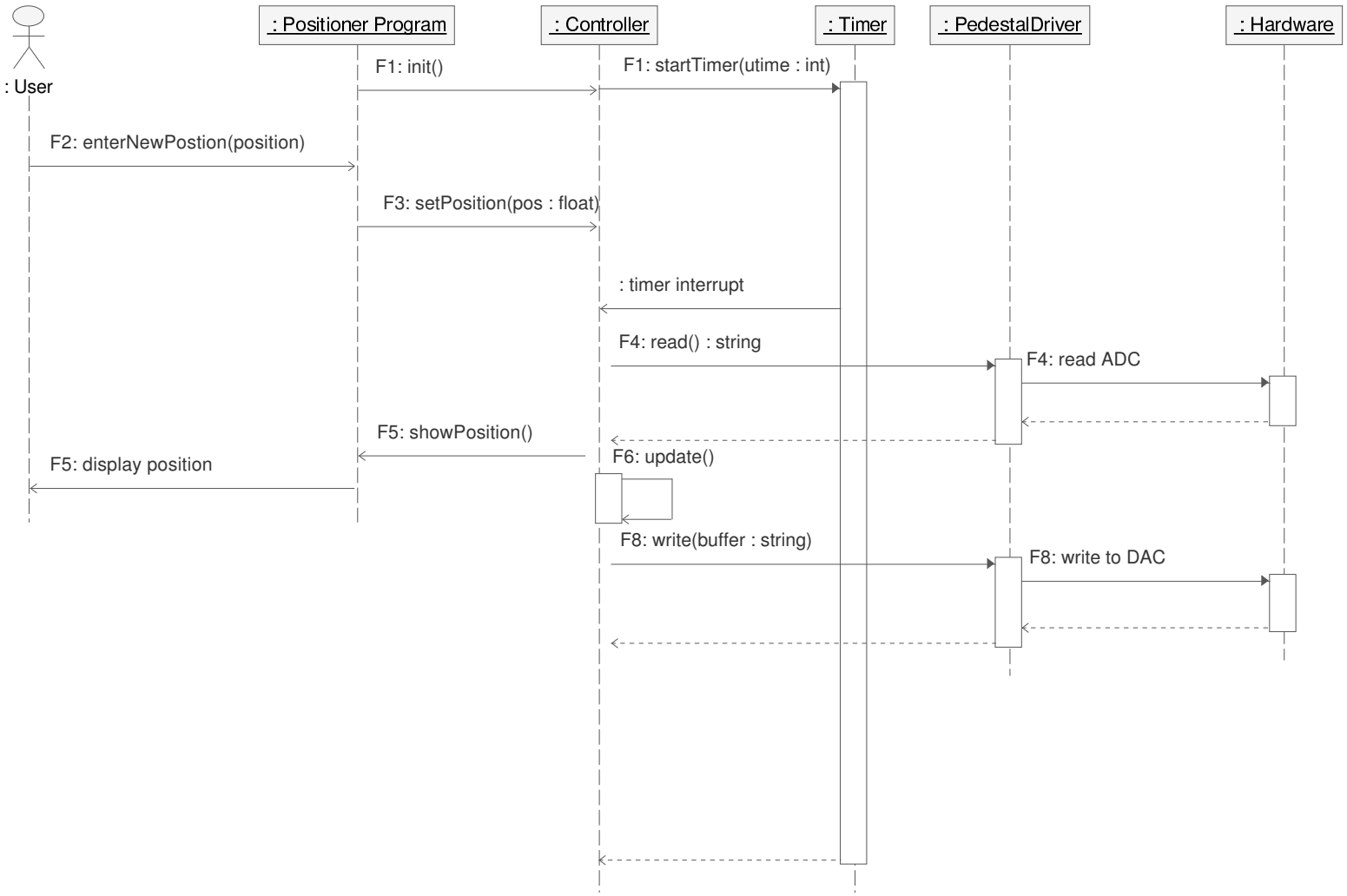Figure 6.7: Flowchart of Position Controller Operation

Figure 6.8: UML Sequence Diagram for Position Controller

Overall

The input of the ADC was connected to the output of the DAC, and the DAC was cycled through the entire range of possible input codes. The input was then compared to the output.

6.4.2   Timer Class

An ISR was constructed that generated a pulse on one of the SBC ports every time it was called. The timer was set to the minimum interrupt time and was initialised to call the ISR whenever a interrupt was generated. The port of the SBC was connected to an oscilloscope and the output waveform was measured.

The timer was then set to generate an interrupt every 100 microseconds and the resulting output waveform was recorded. The waveform was analysed and the frequency and period of the pulse on the waveforms was calculated, to be compared with the specified interrupt time.

6.4.3   Controller Class

The controller class was tested by connecting the entire system except the motors together. The position of the pedestal was held steady, while a new position request was input. The voltage output of the motor drive circuit was expected to climb to the minimum or maximum level and was measured. The pedestal was moved past the new position and the voltage was measured. The voltage was expected to move from either the minimum or maximum level to the other extreme.

Chapter 7

Discussion of Results

This chapter describes the tests done and the results recorded in the actual implementation of the position controller. The chapter deals with each part of the system seperately at first and finally on to the position control system as a whole.

The results discussed in the chapter are for the azimuth axis only, due to a non-functioning elevation motor. However, the same circuit is used for the elevation axis and the motor characteristic are identical, so the results are relevant for both axes.

7.1   Sampling Frequency of the ADC

The ADC driving software was programmed the ADC to convert continuously, in order to measure the maximum achievable sampling rate with this configuration. The timing of the ADC circuit's *busy* convert signal is shown in figure 7.1.

The sampling frequency,f_s, was calculated to be 17.54kHz. , which is more much greater than the required sampling frequency in equation 4.4.

7.2   Resolver Position Conversion

The resolver position circuit was tested in a number of different tests to aid in calculating the overall accuracy, and the over all error in resolving the position is calculated.

7.2.1   Power Supply to Analogue-to-Digital Converter Circuit

The power used to supply the ADC circuit was taken directly from the Cogent CSB337 through the general purpose input output (GPIO) expander, and there was a noise signal
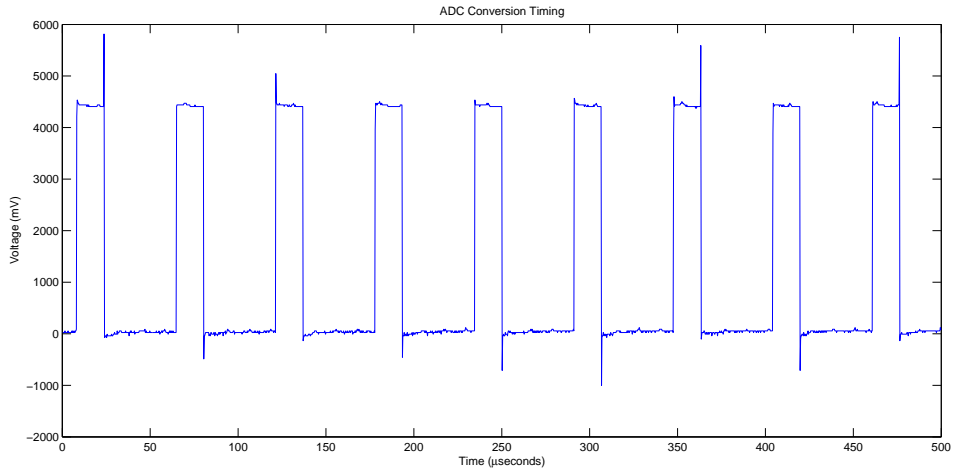
Figure 7.1: ADC *BUSY* Signal

at 100 Hz with a peak-to-peak voltage of 420 mV. A low-pass filter with a -3 dB point of 60Hz was introduced between the power supply and the ADCs. Not all the noise was removed by the filter and the resultant power supply waveform is shown in figure 7.2

The noise is at a frequency of 100 Hz with a peak-to-peak voltage of 131mV, according to the ADC specifications this will cause a degradation of input sensitivity by 3 LSB, therefore the total error in the ADC defined in 4.2 increases to 3 LSB or 19.52 mV, so the effective number of bits (ENOB) of the ADC is 9.
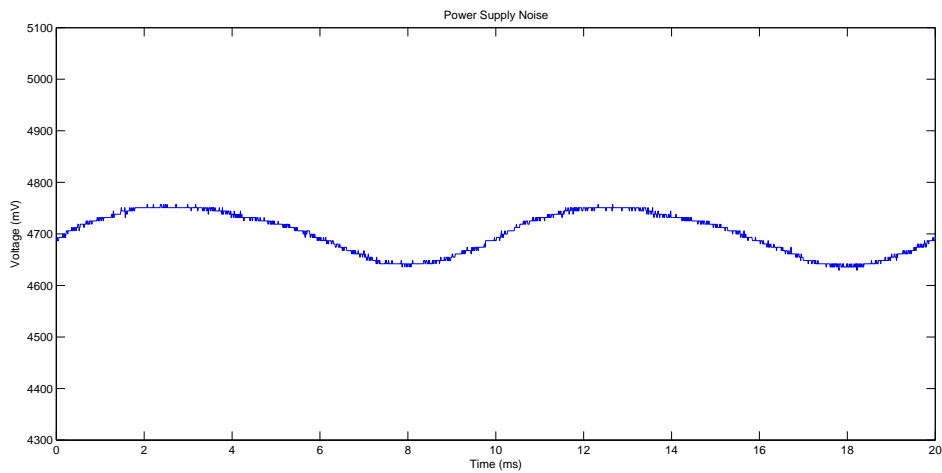

Figure 7.2: Power Supply Noise

7.2.2 Analogue to Digital Conversion Accuracy

The inputs to the ADCs were grounded and 1000 samples were taken, the results are shown in figure 7.3. By examining figure 7.3, it is possible to calculate the effective error

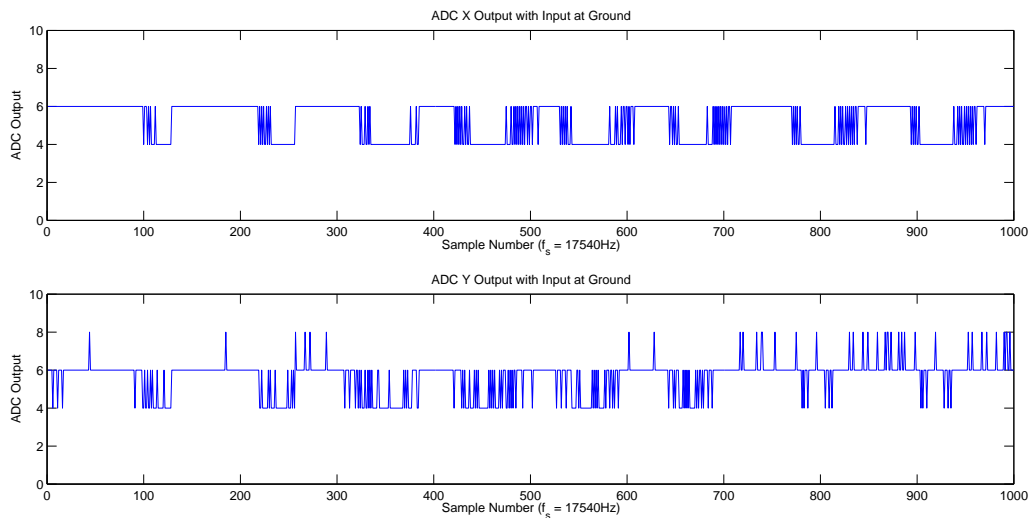of the ADCs, and these values are shown in table 7.1.

Figure 7.3: ADC Output with Inputs at Ground

Table 7.1: ADC Conversion Error

	ADC X	ADC Y
Zero Offset	3 LSB (19.52mV)	3 LSB (19.52 mV)
DC Error	2 LSB (9.76 mV)	4 LSB (39.04 mV)
ENOB	9 bits	8 bits

The position is calculated by the arctan of the ratio of these two voltages as in equation 3.4, so the resultant error in the position is 4 LSB in 16 bits. This means that the resolver conversion has an resolution of 8 bits or 256 levels per 180°. Therefore the effective accuracy of in measuring the position is $\pm 0.7^o$ or 42 arc minutes.

The pedestal was moved with a constant angular rate, and the output of the conversion was measured and is shown in figure 7.4. This shows that the accuracy was indeed within 42 arc minutes.

7.3   Digital to Analogue Conversion Accuracy

To measure the absolute accuracy of the digital to analogue converters, 3 different input codes were tested and the output measured by an oscilloscope, the results are displayed in figure 7.5.

The inputs codes, the expected outputs and the actual outputs are listed in table 7.2. Using these results the maximum error of the DAC circuit is calculated to be:
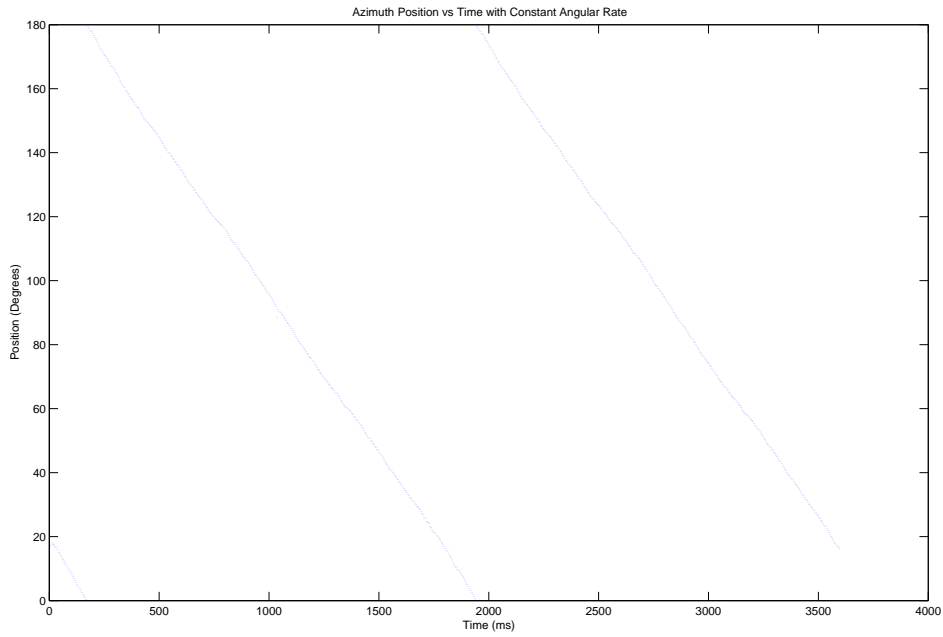
Figure 7.4: Position Output for Constant Angular Rate

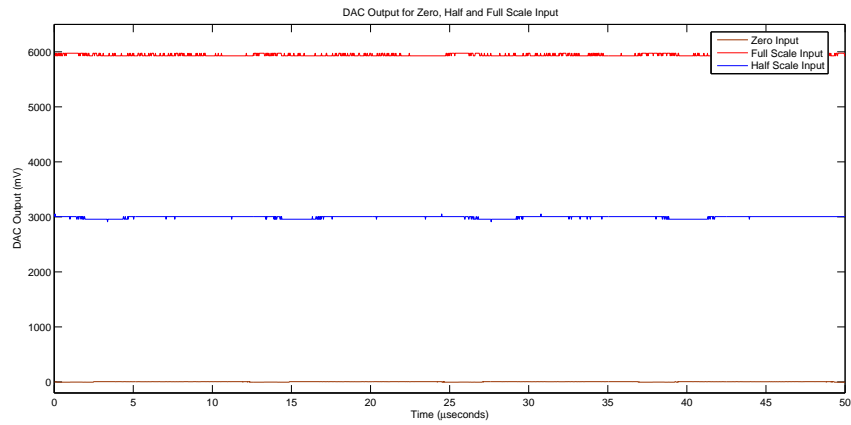Figure 7.5: DAC Output for Different Input Codes

Table 7.2: DAC Performance

Input Code	Expected Output	Actual Output
0	0 V	0 V±0.5%
2047	3 V	2.98 V±0.7%
4097	6 V	5.91 V ±0.7%

$$e_{DAC} = 2.2\% = 132 \text{ mV} \tag{7.1}$$

7.4   Overall Performance of Position Controller

The position controller was installed on the pedestal and the system was given a position 90 degrees from the current position. The rate output on the tachogenerator was recorded by an oscilloscope, the output is shown in figure 7.6.
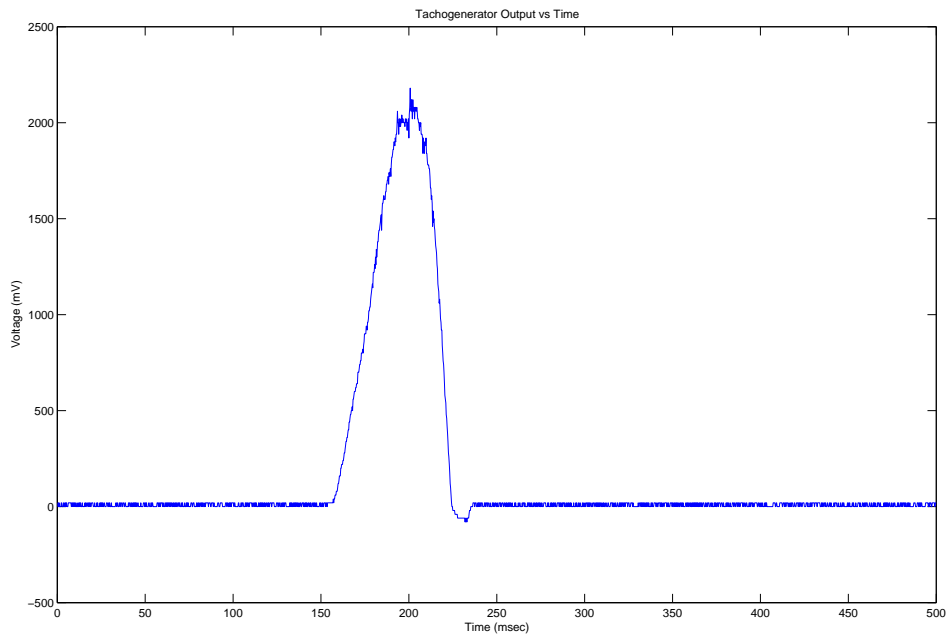

Figure 7.6: Motor Rate for Position Command

Chapter 8

Conclusions and Recommendations

This report demonstrates how a position resolver can be implemented onto a Navy pedestal with an accuracy of 42 arc minutes succesfully, this chapter draws conclusions from the results in the previous chapter, and makes recommendations based on those concusions.

8.1 Position Resolver Accuracy

The accuracy was calculated as 42 arc minutes, and was shown to be within that specification, but for any scientific purposes an antenna controller would need to be more accurate than this.

8.1.1 Recommendations for Improving Accuracy

Regulated Power Supply

The power supply noise would be eliminated by a regulated power supply, and thus reduce the noise on the resolver conversion process.

Printed Circuit Board Design

To eliminate the noise on the resolver conversion, the electronics should be moved to a printed circuit board. The board on which it was designed causes interference and crosstalk with the analogue to digital converter.

Resolver-to-digital Converter

A commercial resolver-to-digital converter could be purchased to replace the ADC circuitery and would offer far superior accuracy.

8.2 Position Controller Performance

Since the focus of this project was not on optimising the performance of the position control loop, the performance of the position controller was examined in great detail. The results of the position controller show that the performance is adequate and this position control system can perform sufficiently well.

8.2.1 Recommendations for Improving Controller Performance

Since the writer of this report has little experience in control systems, an engineer with some experience in this field would possibly be able to improve the performance of this control system remarkably.

Appendix A

Resolver Module

Appendix B

Postioner Application

Bibliography

[1] Tips for using the ADS78xx Family of AD converters. Technical report, Texas Instruments Incorporated, 2000.

[2] *Cogent CSB337 Hardware Reference Manual*, 2003.

[3] D. Abramovitch. Phase-Locked Loops: A Control Centric Tutorial. Technical report, Agilent Labs,Palo Alto, May 2002.

[4] G. Arslan and F. A. Sakarya. Performance Evaluation and Real-Time Implementation of Subspace, Adaptive, and DFT Algorithms for Multi-tone Detection. *Ptolemy Project*, 1996.

[5] K. Banks. The Goertzel Algorithm. *Embedded Systems Programming*, August 2002.

[6] R. Bliss. *Navy Electricity and Electronics Training Series*, 1992.

[7] M. Braae. *Control Theory for Electronic Engineers*. UCT Press, Cape Town, 7700 South Africa, 1994.

[8] A. R. . J. Corbet. *Linux Device Drivers*. O'Reilly Media, Sebastopol, CA 95472, 2001.

[9] J. Gasking. Resolver-to-digital Conversion - A Simple and Cost Effective Alternative to Optical Shaft Encoders. Technical report, Analogue Devices, Massachusetts, March 1992.

[10] J. Horn. ADS7809 TAG Feature. Technical report, Texas Instruments Incorporated, 2000.

[11] P. Horowitz and W. Hill. *The art of electronics*. Press Syndicate of the University of Cambridge, Cambridge,CB2 1RP, 1989.

[12] M. F. Jimmy Mason. Efficient Algorithms and Implementation of a DTMF Detector. Technical report, University of Texas at Austin, 1997.

[13] M. Y. Jin and C. Wu. Servos, Selsyns and Friends. *Tech MusingsIEEE*, 147:1–2, May 2000.

[14] I. P. Johan Lilius. Modelling Embedded Software in UML. Technical report, Abo Akedemi University, 2004.

[15] J. Kessler. *Synchro Resolver Conversion Handbook, Fourth Edition*. Data Device Corporation, Bohemia, NY 11716, 1994.

[16] Y. Y. Z. Z. Lingxia Wang, Bo Yao. A Survey of Embedded Operating Systems, 2000.

[17] M. McClure. A Simplified Approach to dc Motor Modeling for Dynamic Stability Analysis. Technical report, Power Supply Control Products, 2000.

[18] L. C. H. P. M. M.J. Humphreys, D. Brown. *Power Semiconductor Applications*. Philips Semiconductors, Hazel Grove,SK7 4DF, 1994.

[19] N. Morrison. *Introduction to Fourier Analysis*. John Wiley and Sons, Inc, 1994.

[20] A. F. W. G. F. H. J. P. Randy Agosti, Dave Dayton. *Synchro and Resolver Conversion*. Memory Devices Ltd, Surrey, KT8 0SN, 1987.

[21] S. W. Smith. *The Scientist and Engineer's Guide to Digital Signal Processing*. California Technical Publishing, 1997.

[22] G. Thomas. Modelling the Azimuth Position Control System. Technical report, University of Wales Swansea, 2001.

[23] T. Wescott. PID Without a PhD. *Embedded Systems Programming*, October 2000.

[24] J. S. P. W. Wookey, Chris Rutter. *Guide to ARMLinux*. Aleph One, Cambridge, CB5 9BA, 2001.